RL-TR-95-138
Final Technical Report
August 1995

EVALUATION OF GAIN QUENCHING VERTICAL CAVITY LASERS WITH IN-PLANE LASERS FOR SMART PIXEL SWITCHING

Cornell University

D.B. Shire and C.L. Tang

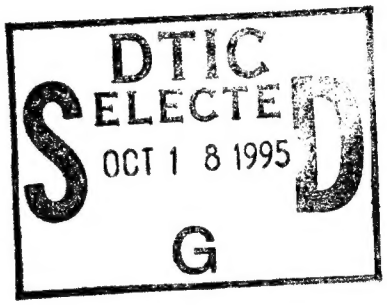

APPROVED FOR PUBLIC RELEASE; DISTRIBUTION UNLIMITED.

Rome Laboratory
Air Force Materiel Command
Griffiss Air Force Base, New York

This report has been reviewed by the Rome Laboratory Public Affairs Office (PA) and is releasable to the National Technical Information Service (NTIS). At NTIS it will be releasable to the general public, including foreign nations.

RL-TR-95-138 has been reviewed and is approved for publication.

APPROVED: Michael A Parker

MICHAEL A. PARKER
Project Engineer

FOR THE COMMANDER: Donald W. Hanson

DONALD W. HANSON
Director of Surveillance & Photonics

If your address has changed or if you wish to be removed from the Rome Laboratory mailing list, or if the addressee is no longer employed by your organization, please notify RL (OCPA) Griffiss AFB NY 13441. This will assist us in maintaining a current mailing list.

Do not return copies of this report unless contractual obligations or notices on a specific document require that it be returned.

REPORT DOCUMENTATION PAGE

Form Approved
OMB No. 0704-0188

1. AGENCY USE ONLY (Leave Blank)	2. REPORT DATE	3. REPORT TYPE AND DATES COVERED
	August 1995	Final Mar 94 - Mar 95

4. TITLE AND SUBTITLE
EVALUATION OF GAIN QUENCHING VERTICAL CAVITY LASERS WITH IN-PLANE LASERS FOR SMART PIXEL SWITCHING

5. FUNDING NUMBERS
C - F30602-94-C-0029
PE - 62702F
PR - 4600
TA - P3
WU - PU

6. AUTHOR(S)
D.B. Shire and C.L. Tang

7. PERFORMING ORGANIZATION NAME(S) AND ADDRESS(ES)
Cornell University
School of Electrical Engineering
Ithaca NY 14853

8. PERFORMING ORGANIZATION REPORT NUMBER
N/A

9. SPONSORING/MONITORING AGENCY NAME(S) AND ADDRESS(ES)
Rome Laboratory (OCPA)
25 Electronic Pky
Griffiss AFB NY 13441-4515

10. SPONSORING/MONITORING AGENCY REPORT NUMBER
RL-TR-95-138

11. SUPPLEMENTARY NOTES
Rome Laboratory Project Engineer: Michael A. Parker/OCPA/(315) 330-7671

12a. DISTRIBUTION/AVAILABILITY STATEMENT
Approved for public release; distribution unlimited.

12b. DISTRIBUTION CODE

13. ABSTRACT (Maximum 200 words)

A detailed study of monolithically integrated, intracavity-coupled in-plane and vertical cavity surface emitting lasers (VCSELs) for smart pixel switching is performed. It is shown that the extent to which the VCSEL section output is quenched depends on the overlap of the two lasers' gain regions, and on the in-plane laser bias current. Complete quenching of the VCSEL output to a small spontaneous emission level is demonstrated under proper operating conditions, as indicated by an upward shift in VCSEL lasing threshold current and by truncation of short pulses. The VCSEL output is an amplified and inverted version of the input signal to the in-plane laser section. The combined device is also shown to be bistable, and an all-optical two-input NOR gate is demonstrated to show the flexibility of this new switching technology. Two in-plane lasers are intracavity-coupled to a common VCSEL section, which serves as the output device. A contrast ratio of at least 5:1 is measured between the logic 0 and logic 1 states. Potential applications of the in-plane/VCSEL smart pixel include free-space interconnects, other all-optical logic gates, and optical memory devices that could be utilized, for example, in an all-optical time slot interchange switch or a dense wavelength division multiplexing (WDM) system.

14. SUBJECT TERMS
Lasers, Smart pixels, Laser quenching, Optical switching

15. NUMBER OF PAGES
36

16. PRICE CODE

17. SECURITY CLASSIFICATION OF REPORT	18. SECURITY CLASSIFICATION OF THIS PAGE	19. SECURITY CLASSIFICATION OF ABSTRACT	20. LIMITATION OF ABSTRACT
UNCLASSIFIED	UNCLASSIFIED	UNCLASSIFIED	UL

Abstract

A detailed study of monolithically integrated, intracavity-coupled in-plane and vertical cavity surface emitting lasers (VCSELs) for smart pixel switching is performed. It is shown that the extent to which the VCSEL section output is quenched depends on the overlap of the two lasers' gain regions, and on the in-plane laser bias current. Complete quenching of the VCSEL output to a small spontaneous emission level is demonstrated under proper operating conditions, as indicated by an upward shift in VCSEL lasing threshold current and by truncation of short pulses. The VCSEL output is an amplified and inverted version of the input signal to the in-plane laser section.

The combined device is also shown to be bistable, and an all-optical two-input NOR gate is demonstrated to show the flexibility of this new switching technology. Two in-plane lasers are intracavity-coupled to a common VCSEL section, which serves as the output device. A contrast ratio of at least 5:1 is measured between the logic 0 and logic 1 states.

Potential applications of the in-plane/VCSEL smart pixel include free-space interconnects, other all-optical logic gates, and optical memory devices which would be utilized, for example, in an all-optical time slot interchange switch or a dense wavelength division multiplexing (WDM) system.

Acknowledgments

The authors wish to thank M. A. Parker, J. S. Kimmet, and R. J. Michalak of Rome Laboratory for their helpful collaboration on this project, and P. D. Swanson, formerly of Rome Laboratory, for developing many of the wafer fabrication process steps used here.

In addition, the authors thank B. Jian, S. Pesarcik, A. Schremer, and the staff of the National Nanofabrication Facility at Cornell University for helpful technical discussions and training.

Table of Contents

List of Figures

I. Introduction

As photonic devices and systems become more extensively used, there is an increasing need to develop the technology to interconnect large numbers of such devices and systems. As the number of devices and systems increases, it will not be practical to have only static interconnections between any two points. It will be necessary to have rapidly re-configurable dynamic interconnections, which is a switching problem. Thus, there are now increasing needs for switching devices and systems for applications ranging from classic circuit switching to fast packet switching and asynchronous transfer mode switching (or asynchronous time-division, etc.)[1] Most of these functions are now still being performed by electronics. Going back-and-forth between the optical and electronic domains adds system complexity with the concomitant added costs and signal degradation. There is, therefore, a clear need for developing an all-optical technology for switching and routing large amounts of information among many nodes for data and telecommunication purposes.

Smart pixels are generally viewed as monolithically integrated devices capable of performing both logic and optical interconnect functions. The logic function might be as simple as one of the Boolean logic operations. Many smart pixels may be combined to form an optical processor. Such a processor can be confined to operate on light traveling in a single 2-D plane; however, the advantages of smart pixel technology may be more fully utilized by interconnecting many signal planes in a stacked, three-dimensional system. Each plane would perform a logical or optical memory function on images impinging on it, then pass the resulting light beams to the next plane for further processing. A need clearly exists, then, for a simple method for transfering an optical signal traveling within the plane of a wafer to a photodetector on another plane. If this function can be performed together with optical logic functions, so much the better.

The vertical cavity surface emitting laser (VCSEL) is an ideal output element for such a smart pixel, owing to the high intensity and low divergence of the output beam. Consequently, a comprehensive study of gain control mechanisms for VCSELs integrated with and intracavity-

coupled to in-plane lasers has been undertaken. The primary reason for this was that there exist a wide range of potential options for modulating the output intensity of in-plane lasers, while comparable intracavity control of stand-alone VCSEL output is difficult due to the short optical cavity and obvious fabrication difficulties. Previous work on gain control of one laser by another intra-cavity coupled laser has involved in-plane lasers only[2-5]. While Uenohara *et al.*[2,3] have demonstrated bistable operation in intersecting in-plane lasers sharing a common saturable absorber region, a fundamental limitation of this approach is the small fraction of the total gain section area which is common to both lasers. Grande *et al.*[4] and Johnson *et al.*[5] used a novel folded-cavity geometry to maximize this overlap in constructing an optical flip-flop. External optical control of VCSEL polarization and wavelength by injection locking has been achieved[6], and VCSEL threshold current has been reduced through external optical feedback[7], but both these scenarios are not obviously compatible with monolithic integration. By contrast, it is a relatively simple matter to integrate in-plane and VCSEL devices in which the VCSEL cavity is completely intersected by the width of the in-plane laser cavity, since the in-plane laser sees the distributed Bragg reflector mirror stacks as composite cladding layers. This work is presented in the following section.

II. Evaluation of Gain Quenching Vertical Cavity Lasers

In this section[8], we discuss the first observation of optical control of the stimulated emission of a VCSEL by an intra-cavity coupled in-plane laser. AlGaAs/GaAs in-plane and VCSELs have been fabricated from the same epitaxial material (Photonics Research Inc. LaseArray VW-850-S-2). A conceptual sketch of the combined device layout is shown in Figure 2.1, with a cutaway section revealing the active layer and a coupling gap. The in-plane laser section is gain-guided and has one end mirror defined by electron cyclotron resonance (ECR) etching[9]. A shallow 1 μm gap in the top p-contact metallization of the lasers separates the in-plane and VCSEL sections. The VCSEL section has a standard ring contact typical of top surface-emitting devices, and its gain region is defined partly by a proton implant and partly (on one side only) by a deep

mirror etch. This 90 degree mirror serves as the other end mirror of the in-plane laser. In other devices, total internal reflection corner mirrors were also found to give adequate performance. The two etch depths are created in a one-step, two-level etching process similar to that used by Johnson *et al.*[5]. A 150 nm thick Ni layer on top of the p-contact metallization serves as the etch mask for the deep BCl_3/Cl_2 ECR etching, and photoresist is used to define the shallow etched areas. After etching the exposed areas to a depth equal to the difference in height between the shallow and deep etched regions, the photoresist mask is removed in an O_2 plasma and etching is subsequently continued until the shallow etch depth (1.5 μm in this case) is reached, and the end mirrors reach their final depth of approximately 4.5 μm. Both the shallow and the deep etched areas were implanted with protons together with the coupling gap region. Last, the wafers were thinned and a NiGeAu ohmic contact was made to the back of the wafer. The alloying step also served to anneal some of the optical damage from the implant. Further details on the processing sequence used to fabricate the devices studied here are given by Parker et al.[10] In this manner, two lasers are created which are capable of being biased independently. The structure is like that of an in-plane laser with a multi-quantum well saturable absorber section, with the important difference that the (VCSEL) section is capable of lasing output in the surface-normal direction. As the driving current to the VCSEL is increased, the power output from the in-plane laser for a fixed in-plane bias current also increases, due to the "saturable absorber" becoming more transparent. It should be noted that an external cavity arrangement in which in-plane laser output was coupled through a polyimide-filled 3 μm gap to an air-post VCSEL device was also implemented. Only minimal effect on VCSEL threshold current was observed in this case, owing to the drastically reduced photon density coupled into the thin VCSEL active region.

Figure 2.2 shows P-I curves of a 20 μm^2 VCSEL for 3 levels of input power from the intra-cavity 20 x 200 μm-long in-plane laser section that it was coupled to. The VCSEL output (together with some scattered light from the in-plane laser section) was measured using a 1 cm diameter Si photodetector mounted approximately 2 cm above the wafer. As the in-plane laser power is increased, the threshold current of the VCSEL increases over 70%. Ultimately, the 20

μm^2 vertical cavity laser will not lase at any current; rather, its spontaneous emission continues increasing until its power output becomes limited by heating. Figure 2.3 shows VCSEL threshold current versus in-plane laser output power for the 20 μm^2 device in Figure 2.2, and a larger, 30 μm^2 device coupled to the same size in-plane laser. It can be seen that while the threshold current in the larger VCSEL increases 30% with increasing in-plane output, even maximum in-plane power is not sufficient to quench the vertical cavity lasing mode. It is believed that this is due to insufficient overlap between the gain regions of the in-plane laser and the (wider) VCSEL. Both devices may lase simultaneously. For low in-plane laser output (below or near threshold), it can also be seen in Figure 2.3 that the VCSEL threshold current initially decreases. This is to be expected, as the situation is similar to a low level of optical pumping from an external laser lowering the lasing threshold by electrical pumping. The high threshold current density of approximately 6,800 A/cm^2 for the VCSELs in this experiment is not believed to be due to inherent limitations imposed by the gain control mechanism shown here. Instead, we believe the cause to be either the highly resistive Bragg reflector stacks in the epitaxial material used, or processing problems; broad area, cleaved facet in-plane lasers fabricated from the same wafer had threshold current densities of only 300-400 A/cm^2. In fact, with improved devices, the gain quenching effects observed should be even more pronounced, particularly with higher power in-plane lasers coupled to smaller VCSELs.

Figures 2.4(a) and 2.4(b) show truncation of the leading edge of a VCSEL output pulse due to an overlapping light pulse from an intra-cavity coupled in-plane laser. The two oscilloscope traces shown in each figure are the voltage input pulse to the in-plane laser section, and the VCSEL output (together with scattered in-plane laser power) as detected above the wafer. In Figure 2.4(a), the in-plane laser output is small, and the VCSEL output pulse, which follows the in-plane laser pulse by 600 nanoseconds, is minimally affected. In Figure 2.4(b), the in-plane laser output is large, and the stimulated emission from the VCSEL during the leading edge of its output pulse is suppressed. In Figure 2.4, the VCSEL was operating just above threshold. If the VCSEL is operated well above threshold, its output is reduced significantly until the in-plane laser pulse ends,

at which point it quickly rises to its nominal power level. During the in-plane laser pulse, the detector output trace ramps up slowly due to a long turn-on delay, possibly another artifact of the materials or processing problems mentioned above. For this reason, the in-plane laser had relatively little impact on the VCSEL output when the leading edge of the in-plane laser pulse overlapped the trailing edge of the VCSEL pulse. This is again believed to be unique to the devices used in this work, and reflects the fact that the in-plane laser had to be well above threshold in order to provide significant gain quenching in the devices studied. Future work will focus on improving the VCSEL and in-plane laser performance to accentuate the effect identified here, and on enlarging the hysteresis in the VCSEL power output vs. in-plane input power characteristic. This is discussed in the following section, together with the results for an all-optical two-input NOR gate.

III. Optical Bistability and NOR-Gate Operation

It has been pointed out that the conditions for bistability in cross coupled lasers depend on the individual lasers' self- and cross-saturation coefficients[11-12]. The cross saturation terms are highest when the overlap of the two lasers' gain sections is maximized. Consequently, the hysteresis in the power output vs. power input characteristic of cross-coupled VCSEL and in-plane lasers is expected to be larger and more easily realized than that observed in cross-coupled in-plane lasers alone. In the cross-coupled in-plane laser case, only a portion of the output laser cavity can be illuminated by the side laser; in the devices discussed here, the VCSEL cavity is completely intersected by the width of its associated in-plane laser(s). We report in this section[13] the first observation of optical bistability in cross-coupled VCSEL and in-plane lasers, and we present an all-optical two-input NOR gate which was fabricated to demonstrate the flexibility of this switching technology.

A conceptual sketch of a 20 μm^2 AlGaAs/GaAs VCSEL integrated with and intracavity coupled to two orthogonal 20x400 μm in-plane lasers A and B is shown in Figure 3.1. The

fabrication of these devices followed the same procedure as the devices discussed in the previous section. Coupling gaps 1 μm wide and 1.5 μm deep are located between the gain sections of the in-plane lasers and the VCSEL (or output) section of the NOR gate. These are proton implanted to allow the in-plane lasers and the VCSEL to be independently biased. Both sections of each in-plane laser are probed and electrically pumped in parallel. As before, the end mirrors of the in-plane lasers are deep-etched to a final depth of 4.5 μm by electron cyclotron resonance (ECR) etching in a BCl_3/Cl_2 plasma.

Figures 3.2(a-c) demonstrate the operation of the NOR gate. In Figure 3.2(a), the lower, abrupt on/off oscilloscope trace is an untruncated 1 μsec voltage input pulse to the VCSEL, with the in-plane laser sections unbiased. The upper trace is the VCSEL output measured with a large area Si photodetector as before. In Figure 3.2(b), the lower trace is a 500 nsec voltage pulse applied to in-plane laser A, and the upper trace again shows the VCSEL output, together with a small amount of scattered light from the in-plane laser. It is clearly seen that when the in-plane laser A is biased above threshold in the logic 1 state, the VCSEL output pulse is truncated (spontaneous emission only, or logic 0) until the time when the in-plane laser is turned off. At that point, the VCSEL output quickly rises to its lasing or logic 1 output level. During this measurement, the orthogonal in-plane laser (B) is off. Figure 3.2(c) shows another scenario, measured using in-plane laser B. The VCSEL is initially in its lasing or logic 1 state. At a later time, the output of in-plane laser B is raised from logic 0 to logic 1, or lasing. The VCSEL output, again shown as the upper trace, is then suppressed to the logic 0 state. If both in-plane lasers are on simultaneously, the VCSEL is quenched even further; however, the scattered light measured at the detector from the in-plane lasers increases. The on/off contrast ratio between the logic states is at least 5:1. As the VCSEL bias is increased to well above threshold, its output is reduced when either of the in-plane lasers is turned on, but the VCSEL continues to lase. In this way, we observe that the on/off contrast ratio reaches a maximum at some VCSEL bias, at which point a further increase in VCSEL current causes the ratio to decrease. The switching speed of the devices discussed here is limited by their large RC charging time constant. The ultimate switching speed in

gain quenched, bistable cross-coupled lasers should be limited by the cavity lifetime, and not by the carrier lifetime as is the case in conventional semiconductor laser operation. The high resistance of the DBR mirrors in the devices studied and their high threshold current of >6000 A/cm^2 limited their operation to pulsed conditions. CW operation and enhanced hysteresis in similar devices prepared from higher quality epitaxial material are now being pursued in our laboratory.

Figure 3.3 shows the hysteresis in the power output vs. power input characteristic of a 20 μm^2 VCSEL intracavity-coupled to a 20x600 μm in-plane laser. The data may be interpreted as follows. In the upper portion of the loop, the VCSEL is lasing, and the in-plane laser is off. As the top of the loop is traversed from left to right, the VCSEL output initially increases. Here, the spontaneous emission from the in-plane laser optically pumps the VCSEL and decreases its threshold current. Eventually, the light output of the in-plane laser increases rapidly as it begins to lase at P_1, and the VCSEL output is suppressed. The VCSEL output is reduced to below 0.05 mW of spontaneous emission when the in-plane laser is at full output. When the in-plane laser power is reduced, the VCSEL remains off until P_2 is reached, at which point the VCSEL begins to turn on once again. The observed hysteresis loop is approximately 20 mA wide, from inspection of the in-plane current axis of Figure 3.3. To ensure that the VCSEL output only was being measured, the scattered light from the in-plane laser was measured separately and subtracted from the combined in-plane and VCSEL output signal measured with the large-area photodetector. The in-plane laser power itself was measured using a reverse-biased vertical-cavity p-n photodetector fabricated adjacent to the in-plane laser output mirror and coupled through a polyimide-filled 3 μm gap.

It is seen in both Figures 3.2 and 3.3 that the in-plane laser is more effective at quenching the VCSEL output when it is turned on prior to the VCSEL than when the opposite is true. This is attributed to the in-plane laser dramatically increasing the VCSEL threshold current with increasing output above the in-plane laser threshold. This effect was also found to depend on the overlap of the cavities of the in-plane and vertical cavity lasers. The absence of VCSEL bias increases the in-

plane threshold somewhat also, since that section of the in-plane laser cavity acts in that case as a saturable absorber.

IV. Device Applications and Conclusions

Applications for the intra-cavity coupled laser smart pixel include other integrated all-optical logic gates and inverters, optical interconnection between signal planes with low-divergence output beams, and sources and optical memory elements for dense wavelength division multiplexed (WDM) switching networks or time slot interchange circuits. The technology is compatible with existing, monolithic photonic integrated circuit (PIC) fabrication methods involving in-plane lasers only, and it is very flexible. For example, an analog or digital input signal may be amplified by a main in-plane laser with multiple intra-cavity VCSEL sections, as shown in Figure 4.1. The wavelength or the time slot of the output signal may then be chosen by turning off the side in-plane laser coupled to the desired VCSEL, thereby allowing that VCSEL to lase. This transfers the inverted and amplified input signal to the VCSEL's output. The bistability of the coupled laser pair may also be used to advantage by incorporating such elements as buffers or latches for optical memory, an important component of a time slot interchange sytem such as that shown in Figure 4.2.

In conclusion, we have demonstrated the first observation of optical control of the stimulated emission of a vertical cavity surface emitting laser (VCSEL) by an intra-cavity coupled in-plane laser. Bistability and all-optical NOR gate operation in similar devices fabricated from the same epitaxial material are also reported for the first time. Depending on the overlap between the two gain regions and the laser bias currents, complete quenching of the VCSEL's stimulated emission is observed, and hysteresis exists in the VCSEL power output vs. in-plane power input characteristic. The combined device offers a wide variety of potential smart pixel applications including integrated all-optical logic gates and inverters, optical interconnects, and sources and optical memory elements for dense WDM switching networks and time slot interchange circuits.

REFERENCES

1. *Photonics in Switching*, edited by J. E. Midwinter (Academic Press, New York, 1993).

2. H. Uenohara, Y. Kawamura, H. Iwamura, K. Nonaka, H. Tsuda, and T. Kurokawa, Electron. Lett. **28**, 1973 (1992).

3. H. Uenohara, Y. Kawamura, H. Iwamura, K. Nonaka, H. Tsuda, and T. Kurokawa, Electron. Lett. **29**, 609 (1993).

4. W. J. Grande, J. E. Johnson, and C. L. Tang, Appl. Phys. Lett. **57**, 2537 (1990).

5. J. E. Johnson, W. J. Grande, and C. L. Tang, Appl. Phys. Lett. **63**, 3273 (1993).

6. Z. G. Pan, S. Jiang, M. Dagenais, R. A. Morgan, K. Kojima, M. T. Asom, R. E. Leibenguth, G. D. Guth, and M. W. Focht, Appl. Phys. Lett. **63**, 2999 (1993).

7. S. Jiang, Z. Pan, M. Dagenais, R. A. Morgan, and K. Kojima, IEEE Photonics Technol. Lett. **6**, 34 (1994).

8. D. B. Shire, M. A. Parker, P. D. Swanson, J. S. Kimmet, and C. L. Tang, Appl. Phys. Lett., **66**, 1717 (1995).

9. P. D. Swanson, D. B. Shire, C. L. Tang, M. A. Parker, J. S. Kimmet, and R. J. Michalak, IEEE Photonics Technol. Lett., June, 1995, accepted for publication.

10. M. A. Parker, J. S. Kimmet, S. I. Libby, and P. D. Swanson, USAF Technical Report #RL-TR-94-103, August, 1994.

11. C. L. Tang, A. Schremer, and T. Fujita, Appl. Phys. Lett., **51**, 1392 (1987).

12. H. Kawaguchi, *Bistabilities and Nonlinearities in Laser Diodes* (Artech House, London, 1994).

13. D. B. Shire, M. A. Parker, and C. L. Tang, Elect. Lett., March, 1995, submitted for publication.

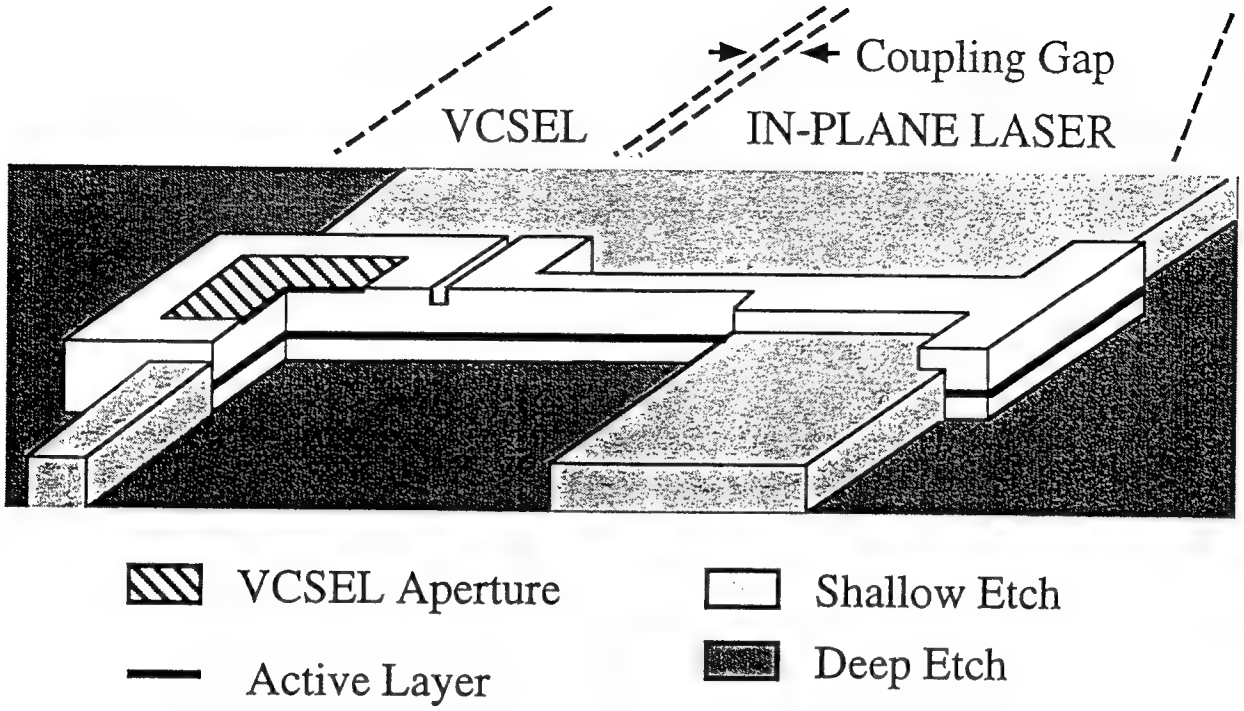

2.1. Conceptual sketch of an in-plane laser with an intra-cavity coupled vertical-cavity surface emitting laser section. A cutaway section reveals a shallow-etched, proton-implanted 1 μm coupling gap, and the combined device's active layer. The end mirrors of the in-plane laser are deep etched to a depth of 4.5 μm.

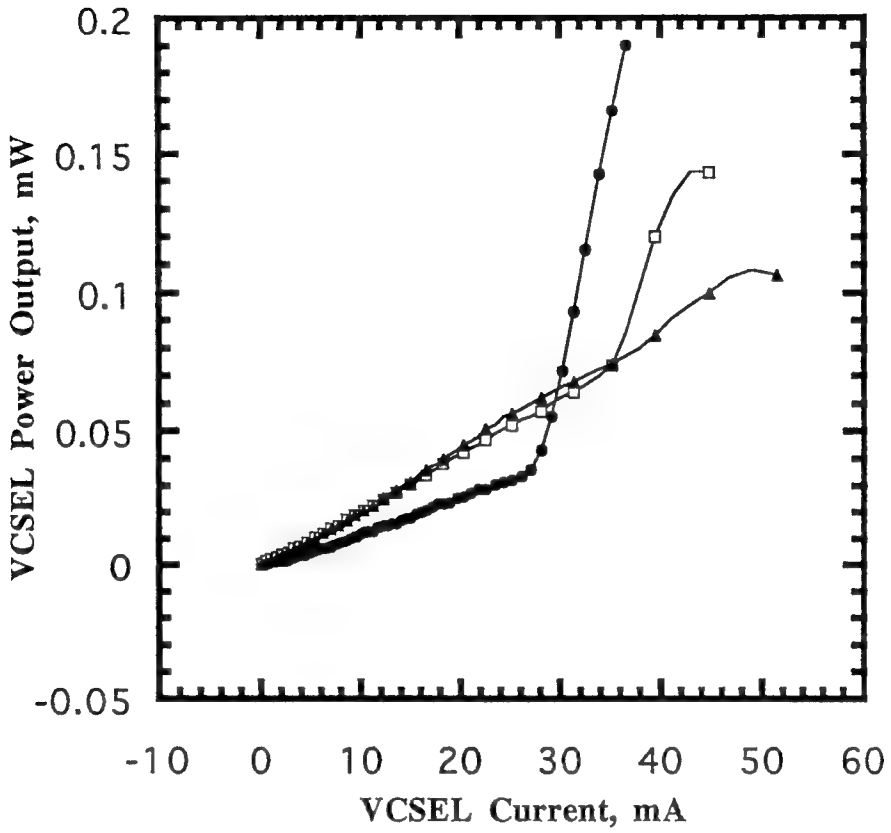

2.2. P-I curves for a 20 μm^2 VCSEL with (●) 0 input power from a 20x200 μm intra-cavity coupled in-plane laser, (◻) 75% of maximum in-plane laser power, (▲) maximum in-plane power.

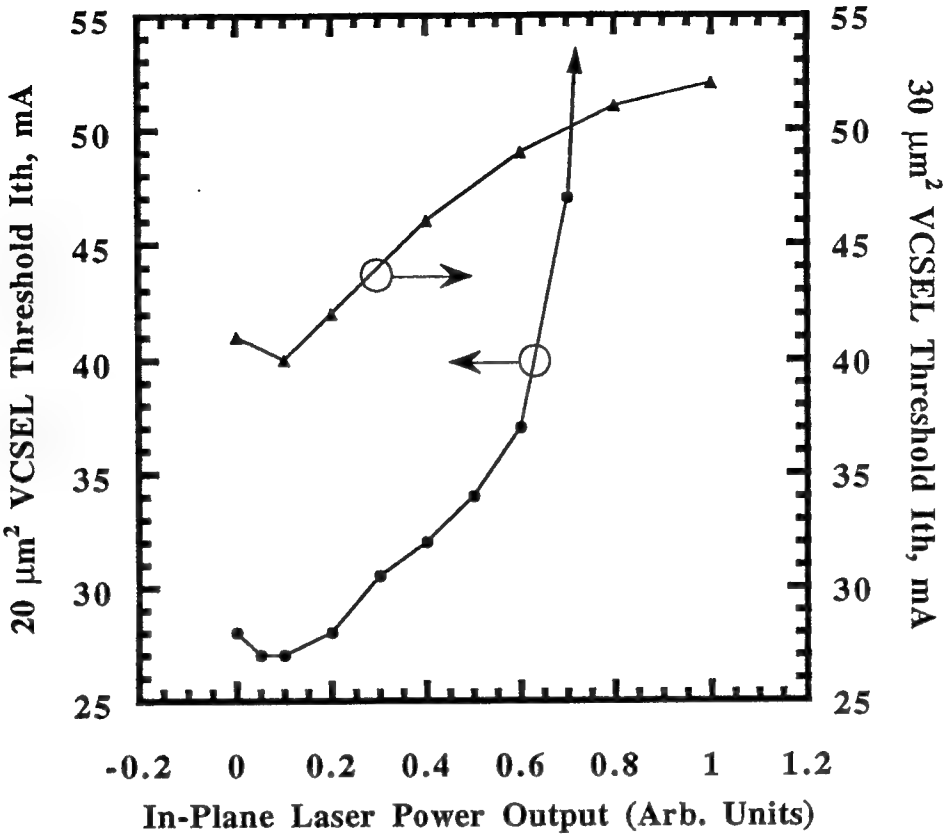

2.3. Threshold current in (●) a 20 μm^2 VCSEL and (▲) a 30 μm^2 VCSEL versus output power in the 20x200 μm intra-cavity in-plane laser they were coupled to. The in-plane power was measured with no pumping in the VCSEL region by a reverse biased vertical cavity p-n photodetector fabricated adjacent to the in-plane laser and coupled through a polyimide-filled 3 μm gap.

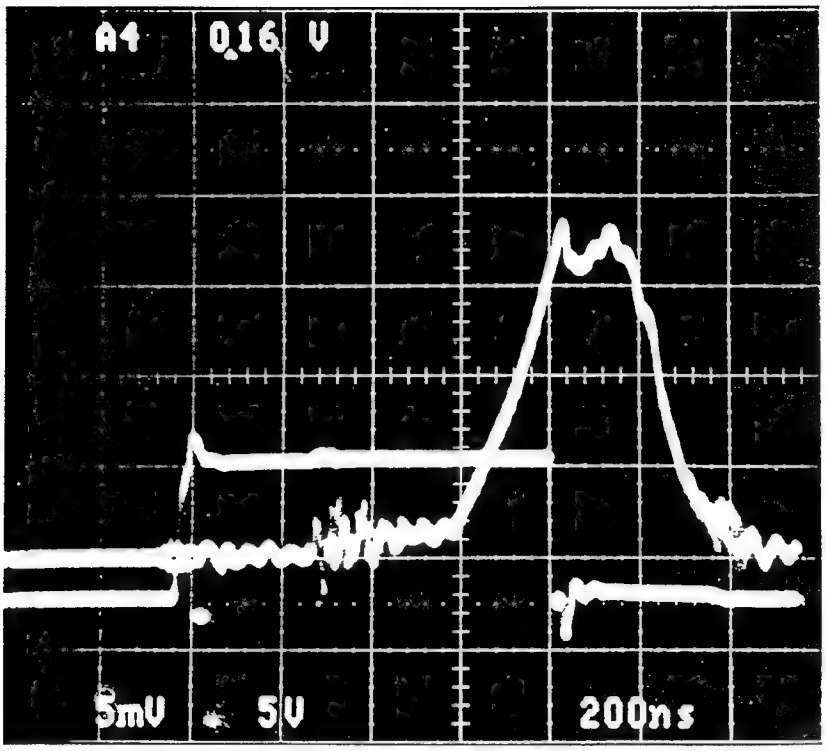

2.4(a) Left, abrupt on/off trace: voltage input to the intra-cavity in-plane laser section. Right trace: power output detected above the wafer. The VCSEL output pulse trails the in-plane laser pulse by 600 nanoseconds.

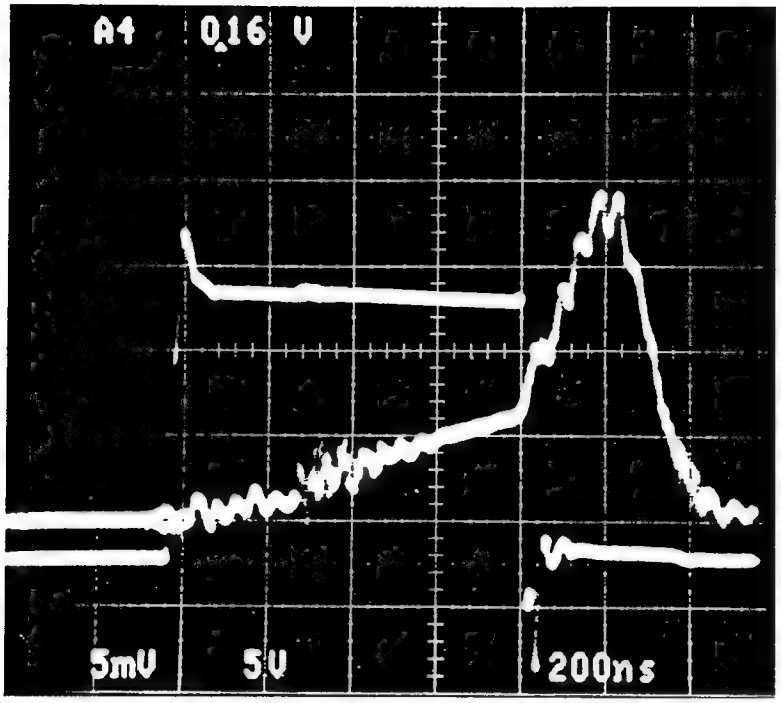

2.4(b) Same as (a), but in-plane laser power increased. Note the truncation of the leading edge of the VCSEL output pulse, which follows the in-plane laser pulse.

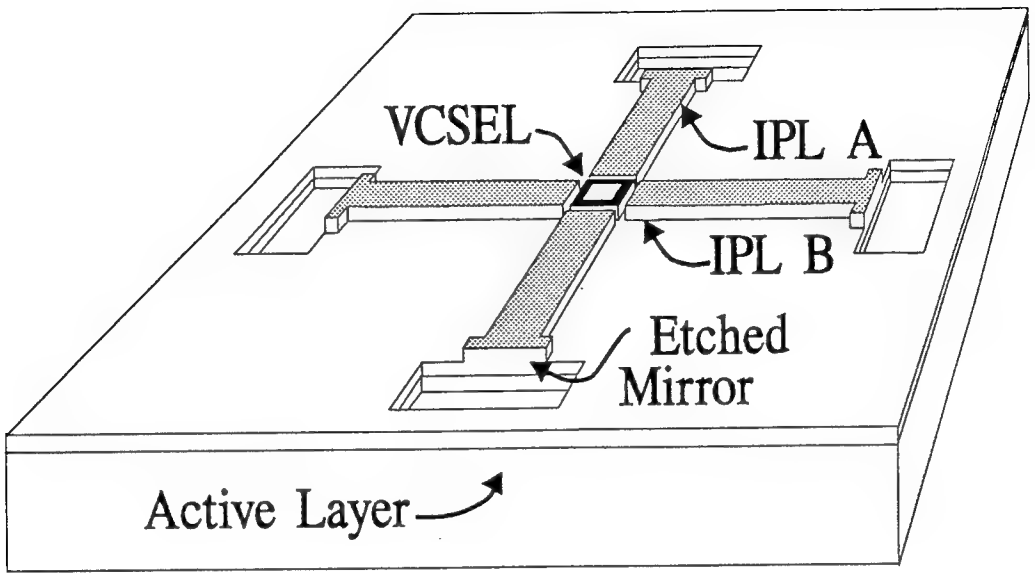

3.1 Conceptual sketch of the all-optical NOR gate

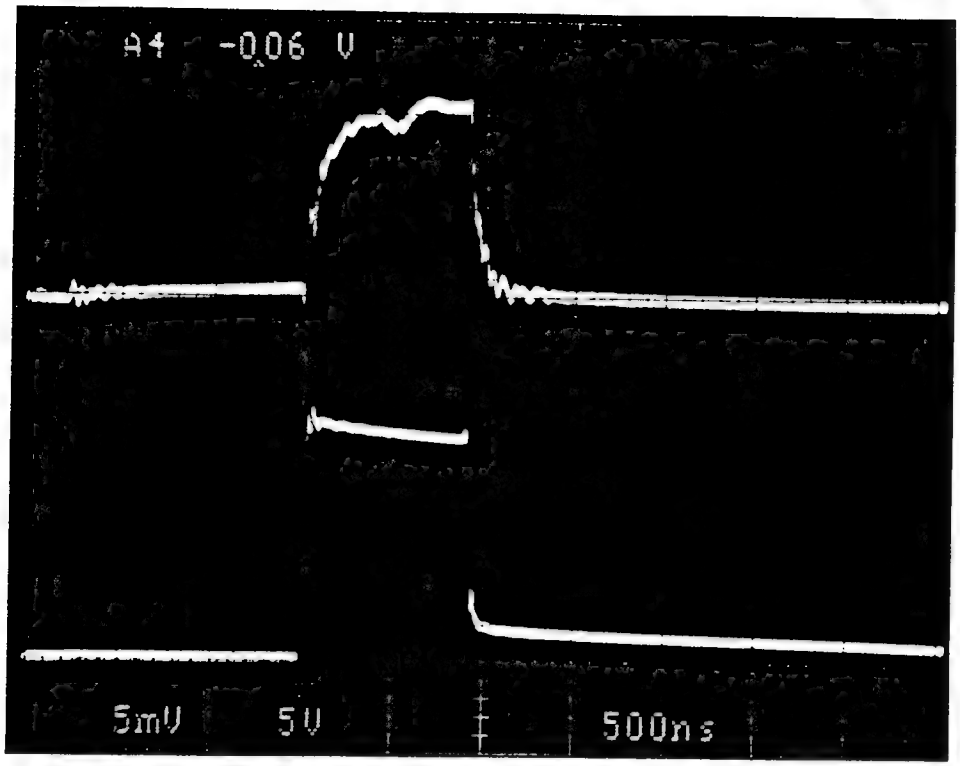

3.2 Oscilloscope traces showing NOR gate operation. (a) Upper trace: 1 μsec VCSEL output pulse. Lower trace: VCSEL input voltage pulse.

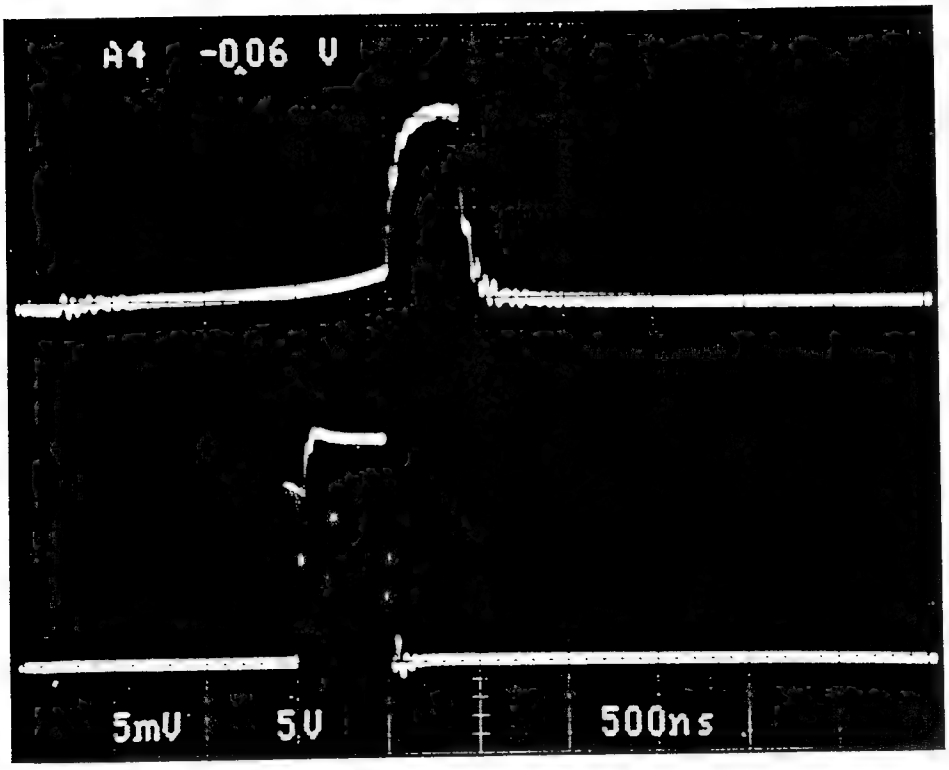

Figure 3.2(b) Upper trace: truncated VCSEL output due to quenching.

Lower trace: in-plane laser A input voltage pulse.

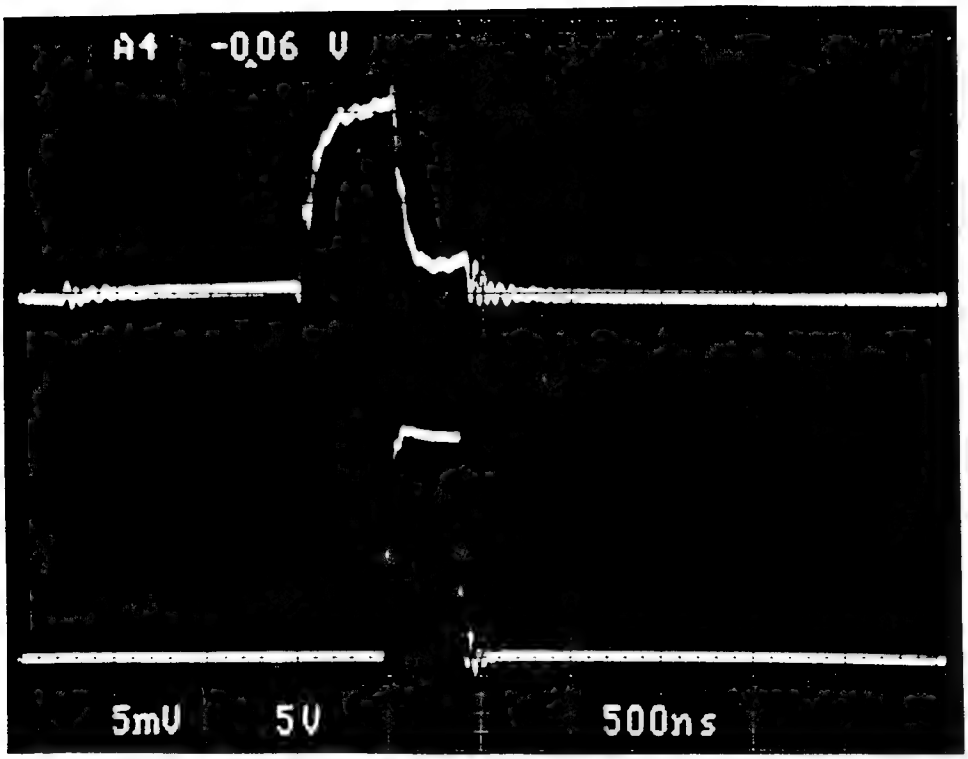

Figure 3.2(c) Upper trace: truncated VCSEL output due to quenching.

Lower trace: in-plane laser B input voltage pulse.

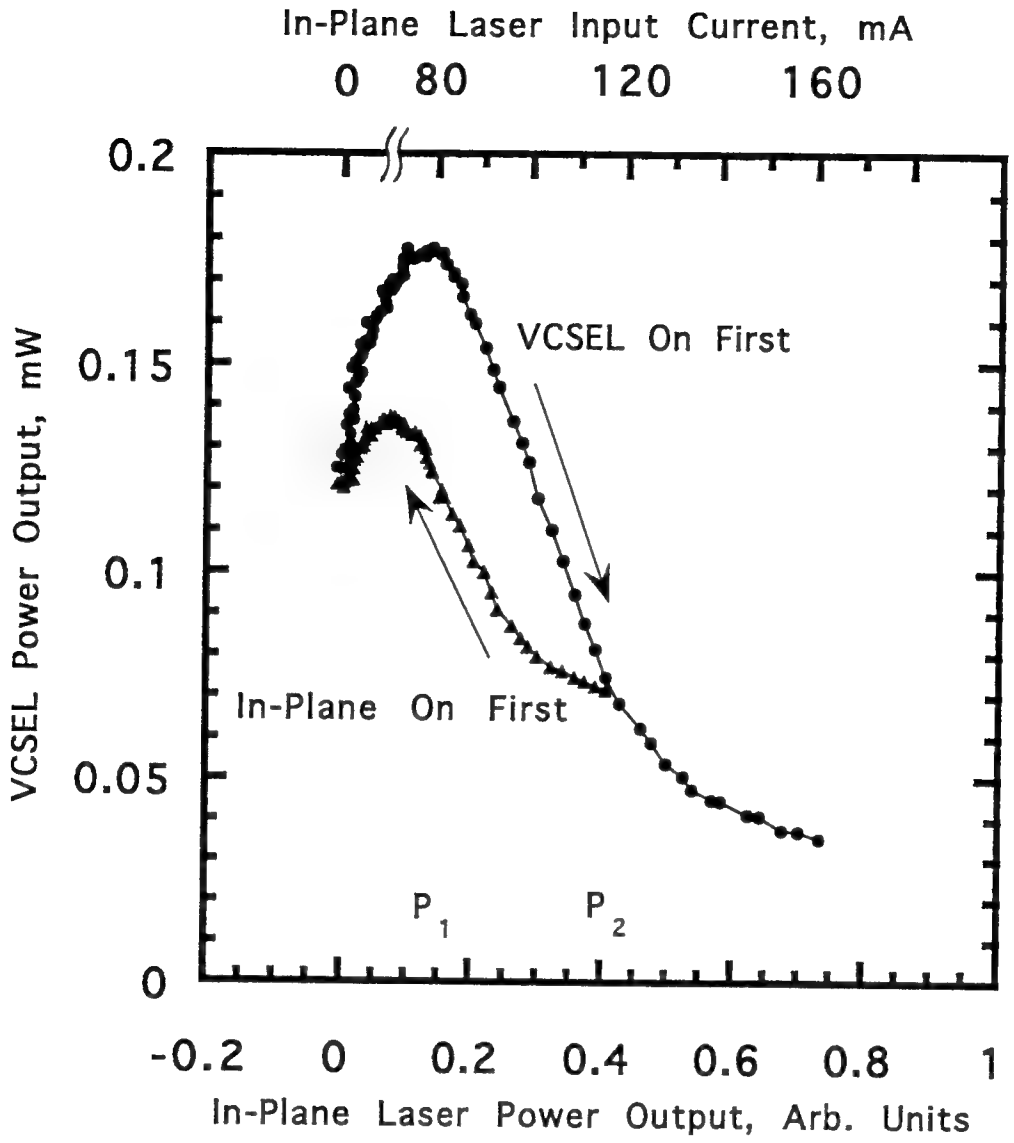

3.3 Optical bistability in intracavity-coupled in-plane and vertical cavity lasers. (●) VCSEL lasing first, in-plane power output increasing; (▲) In-plane laser on first, in-plane power output decreasing.

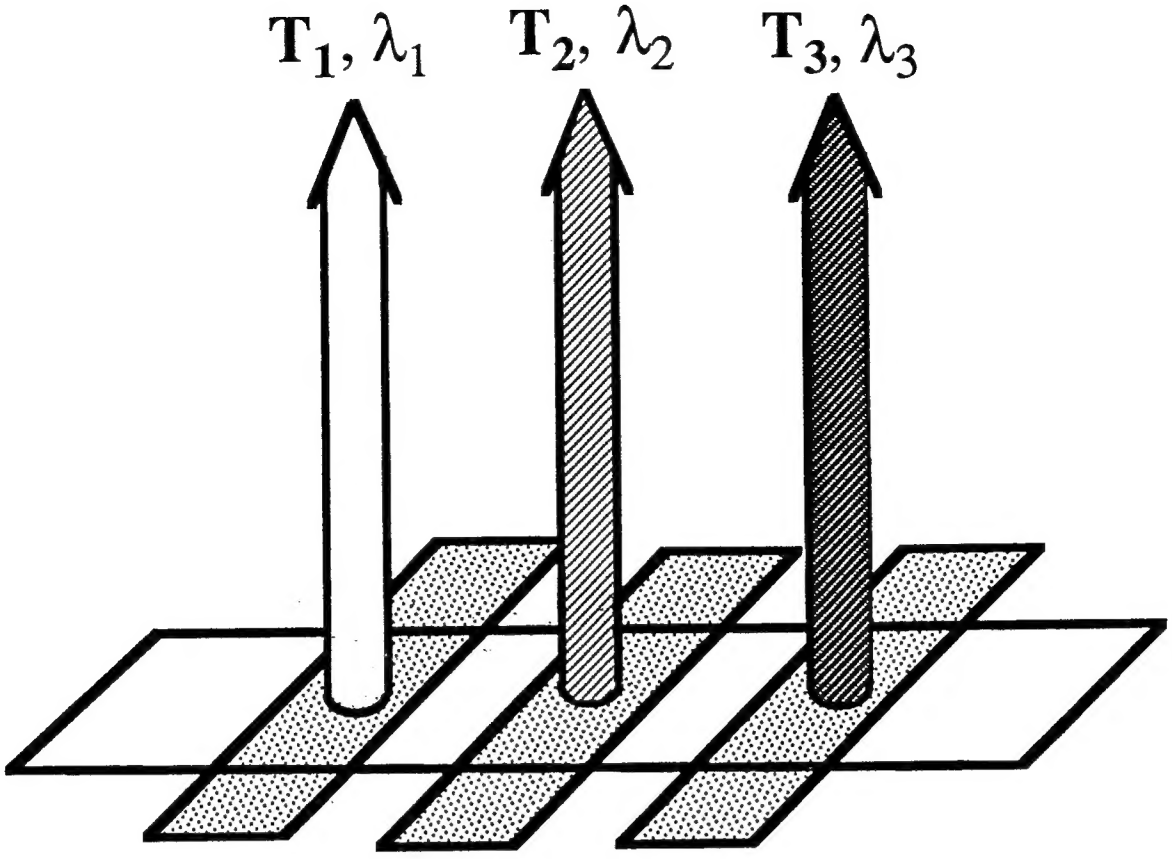

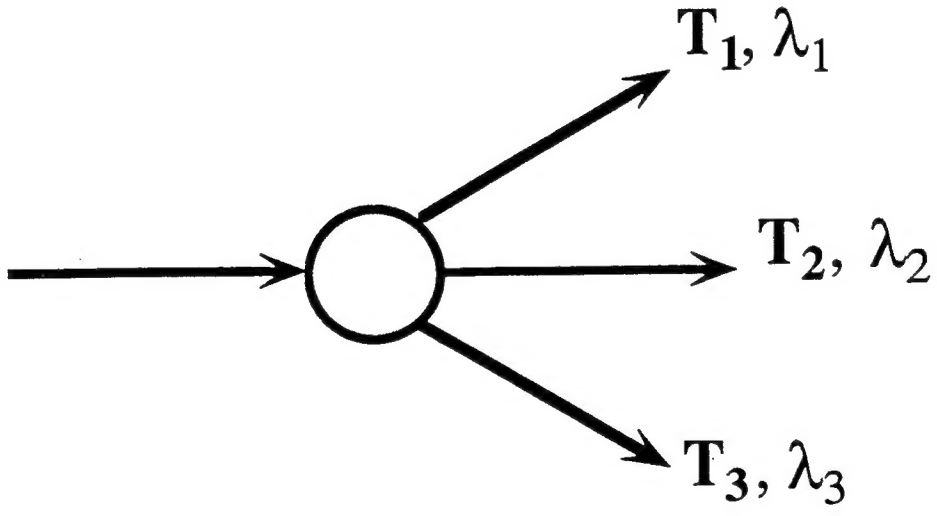

4.1 An in-plane laser with multiple intracavity VCSEL sections (each of which is controlled by a separate side in-plane laser) may function as a 1xN space division switch or as the source in a dense WDM system.

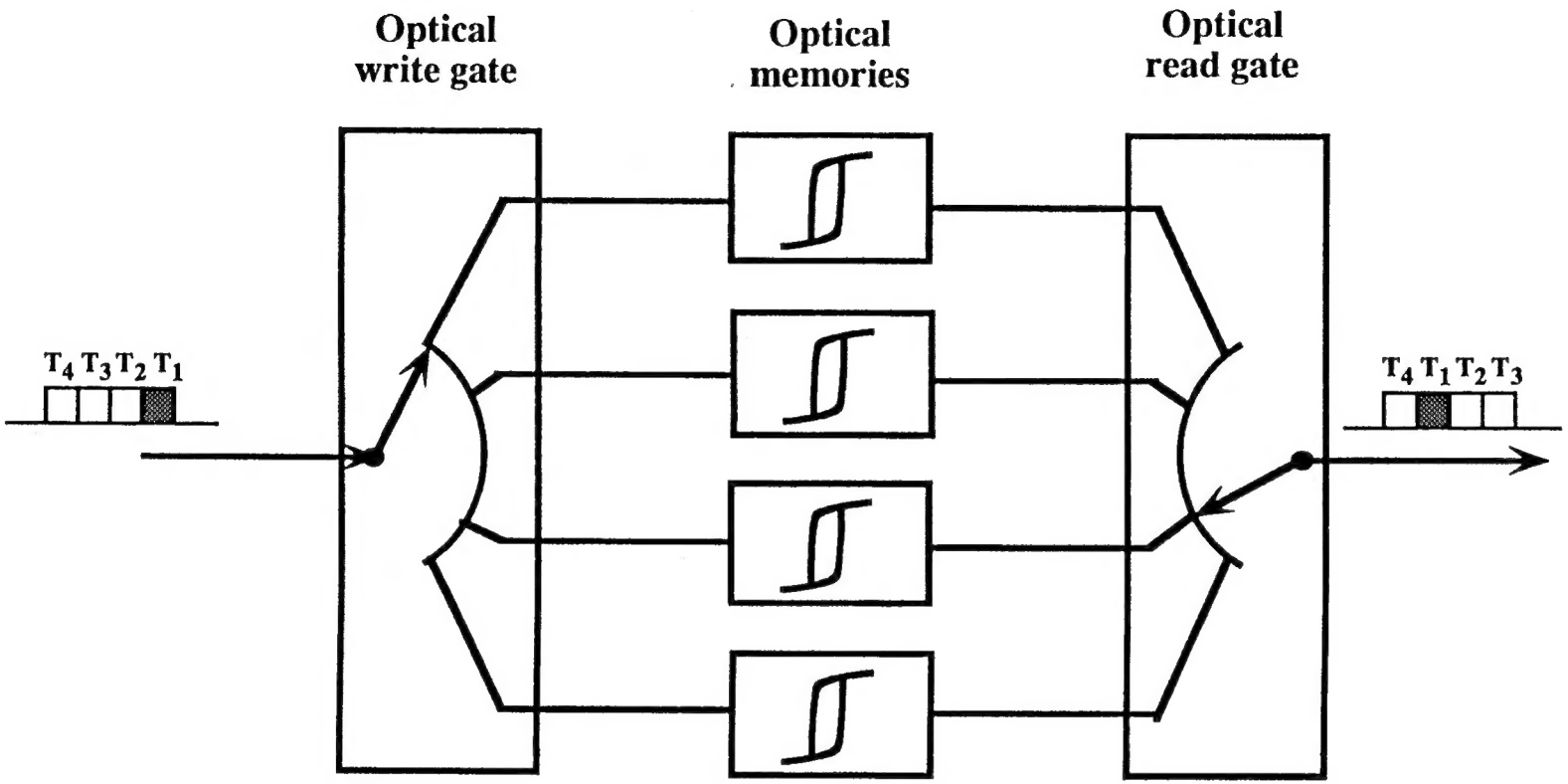

4.2 Schematic diagram of an all-optical time-division switch.

Rome Laboratory

Customer Satisfaction Survey

RL-TR-_____

Please complete this survey, and mail to RL/IMPS, 26 Electronic Pky, Griffiss AFB NY 13441-4514. Your assessment and feedback regarding this technical report will allow Rome Laboratory to have a vehicle to continuously improve our methods of research, publication, and customer satisfaction. Your assistance is greatly appreciated.
Thank You

_____

_____

Organization Name:_____(Optional)

Organization POC: _____(Optional)

Address:_____

1. On a scale of 1 to 5 how would you rate the technology developed under this research?

5-Extremely Useful 1-Not Useful/Wasteful

Rating_____

Please use the space below to comment on your rating. Please suggest improvements. Use the back of this sheet if necessary.

2. Do any specific areas of the report stand out as exceptional?

Yes___ No_____

If yes, please identify the area(s), and comment on what aspects make them "stand out."

3. Do any specific areas of the report stand out as inferior?

Yes___ No___

If yes, please identify the area(s), and comment on what aspects make them "stand out."

4. Please utilize the space below to comment on any other aspects of the report. Comments on both technical content and reporting format are desired.

*U.S. GOVERNMENT PRINTING OFFICE: 1995-610-126-20022